PNAS RESEARCH ARTICLE | CELL BIOLOGY

Dysregulation of PD-L1 by UFMylation imparts tumor immune evasion and identified as a potential therapeutic target

Junzhi Zhou[a,1,2], Xiaohe Ma[a,1], Xingrui He[b], Beiying Chen[a], Jiao Yuan[c], Zhemin Jin[d], Lijing Li[d], Zhiguo Wang[a], Qian Xiao[e], Yafei Cai[f], and Yongkang Zou[g,2]

Edited by Aaron Ciechanover, Technion Israel Institute of Technology The Ruth and Bruce Rappaport Faculty of Medicine, Haifa, Israel; received September 14, 2022; accepted January 18, 2023

Immunotherapy of PD-L1/PD-1 blockage elicited impressive clinical benefits for cancer treatment. However, the relative low response and therapy resistance highlight the need to better understand the molecular regulation of PD-L1 in tumors. Here, we report that PD-L1 is a target of UFMylation. UFMylation of PD-L1 destabilizes PD-L1 by synergizing its ubiquitination. Inhibition of PD-L1 UFMylation via silencing of UFL1 or Ubiquitin-fold modifier 1 (UFM1), or the defective UFMylation of PD-L1, stabilizes the PD-L1 in multiple human and murine cancer cells, and undermines antitumor immunity in vitro and mice, respectively. Clinically, UFL1 expression was decreased in multiple cancers and lower expression of UFL1 negatively correlated with the response of anti-PD1 therapy in melanoma patients. Moreover, we identified a covalent inhibitor of UFSP2 that promoted the UFMylation activity and contributed to the combination therapy with PD-1 blockade. Our findings identified a previously unrecognized regulator of PD-L1 and highlighted UFMylation as a potential therapeutic target.

post-translational modification | UFMylation | PD-L1 | immune checkpoint | tumor immunity

Significance

Cancer cells utilize the expression of PD-L1 to evade $CD8^+$ T cell-mediated immune surveillance. A better understanding of the molecular regulation of PD-L1 expression may contribute to the success of anti-PD-L1/PD-L1 therapies in patients with low response and resistance to immune checkpoint blockade (ICB) therapy. Here, we reported that PD-L1 is a unique target for UFMylation. Decreased expression of UFL1 reduces the UFMylation of PD-L1, which stabilizes PD-L1 and imparts immune evasion. A covalent inhibitor of UFSP2 could promote the UFMylation of PD-L1 and destabilizes PD-L1, leading a tumor-suppressive effect in tumor mouse model. We provided a unique connection between PD-L1 and protein modification by Ubiquitin-fold modifier 1 (UFM1) (UFMylation).

The ubiquitin and ubiquitin-like protein systems control many cellular functions and the dysregulation of those modifications was associated with the development of human cancers (1). The increasing recognition of the fundamental importance of these pathways in physiology and pathology has promoted the application of small molecules to selectively block the functions of these pathways in tumors (2). Ubiquitin-fold modifier 1 (UFM1) is a ubiquitin-like modification with low percentage of sequence homology compared with other ubiquitin and ubiquitin-like molecules (3). Unlike ubiquitination which encompasses several E1s, dozens of E2s (>50), and hundreds of E3s (>600), the UFM1 modification (UFMylation) is catalyzed by the dynamic enzymatic reaction with unique E1 (UBA5), E2 (UFC1), and E3 (UFL1) and finally, UFM1 is covalently added to the Lys residues of targets (3). The proteases UFM1-specific cysteine proteases 1 (UFSP1) and 2 (UFSP2) execute the maturation of the UFM1 precursor and UFSP2 has long been considered the only functional UFSP in humans (4, 5). Recently, it has been reported that human UFSP1 is also an active UFM1-specific protease that regulates UFM1 maturation and UFMylation activity (6, 7). The satellite components DDRGK1 and CDK5RAP3 were considered key regulators of the UFMylation system (8–10). It has been identified that gene variants of the UFMylation components contributed to the neurodevelopmental diseases and demonstrated the potential involvement of UFMylation components in other human disease models, such as microcephaly, atherosclerosis, steatohepatitis, ischemic heart injury, and type two diabetes (11–15). A growing number of studies have revealed that UFMylation plays a critical role in genomic instability (16–19), protein synthesis, endoplasmic reticulum (ER) homeostasis, and other diverse cellular processes (5, 8, 10, 20–29). Recently, it has been shown that UFMylation components play roles in regulating responses to IFN-γ–activated macrophages and plasma cell development, suggesting that UFMylation components may protect cells from external pathogen in a manner of innate or adaptive immune responses (24, 30). So far, only a few substrates of UFMylation have been described. The substrates of the UFMylation and its underlying biological significance, especially in tumorigenesis and tumor microenvironment, have remained poorly understood.

The programmed cell death protein 1 pathway (PD-1/PD-L1) is the most intensively studied negative regulatory checkpoint pathway which inhibits proliferation and activation of $CD8^+$ T cells and imparts tumor cells to evade immune surveillance (31–33). It has been reported that antibodies against PD-L1/PD-1 have elicited a durable response in a subset of patients with a broad spectrum of cancers (melanoma, non-small cell lung cancer, head-and-neck cancer, urothelial carcinoma, high microsatellite instability colorectal carcinoma, Hodgkin's lymphoma, etc.) (32, 34–38), and the high-level expression of PD-L1

Author contributions: J.Z. and Y.Z. designed research; J.Z., X.M., B.C., Z.J., L.L., and Y.Z. performed research; J.Z., X.H., J.Y., Z.W., Q.X., Y.C., and Y.Z. analyzed data; and J.Z. and Y.Z. wrote the paper.

Competing interest statement: The authors have patent filings to disclose, J.Z. and Y.Z. were listed as inventors on a patent owned by the Hangzhou Normal University related to this work.

This article is a PNAS Direct Submission.

[1]J.Z. and X.M. contributed equally to this work.

[2]To whom correspondence may be addressed. Email: zhoujunzhi2013@163.com or zouyk@szbl.ac.cn.

This article contains supporting information online at https://www.pnas.org/lookup/suppl/doi:10.1073/pnas.2215732120/-/DCSupplemental.

Published March 9, 2023.

in tumors has been considered as a biomarker of response for anti-PD1/PD-L1 therapies (39). Thus, revealing the underlying mechanisms of how PD-L1 is regulated in tumor cells may contribute to immune checkpoint blockade (ICB) therapy. PD-L1 expression is critically controlled at both the transcriptional and posttranslational levels in normal tissues under intrinsic and extrinsic stresses to prevent tissue inflammation and contribute to homeostasis maintenance (40–42). However, cancer cells utilize the aberrant expression of PD-L1 to evade immune surveillance (43). Recent studies revealed the mechanisms that posttranslational modifications, such as ubiquitination (44), glycosylation (45), phosphorylation (46), acetylation (47), and palmitoylation (48, 49), regulate the stability of PD-L1 and eventually affect the cancer immune surveillance. Inhibitors of CSN5 and HDAC2, identified as the posttranslational modification regulators of PD-L1, can reduce PD-L1 stability and nuclear localization, respectively, providing an effective approach for combinational therapy with the help of immune checkpoint therapy (41, 44, 47). PD-L1 is both a membrane and exosome protein, which was synthesized and glycosylated on ER (45, 50–52). Except for glycosylation, the mechanism of how PD-L1 is being modified at posttranslational level within ER remains incompletely known (42, 45, 53). Emerging evidence revealed that the ER-resident UFMylation plays an essential role in ER homeostasis (8, 24, 25, 54). We recently reported that UFMylation family genes have high frequencies of somatic copy number alterations and the copy number loss of UFL1 in a multiple cancer types (18), which means dysregulation of UFMylation may lead to a wide range of effects on ER. Therefore, we are curious whether dysregulation of UFMylation affects the biological functions of PD-L1.

Here, we report that PD-L1 is a unique target of UFMylation. Reduced expression of UFL1 decreases the UFMylation of PD-L1 and maintains the PD-L1 stability by antagonizing its ubiquitination, which interdicts $CD8^+$ T cell-mediated antitumor immunity. Thus, our findings identified that UFMylation is a posttranslational modification of PD-L1 and highlighted UFMylation as a potential therapeutic target in tumors.

Results

High Expression of UFL1 Was Associated with Immune-Active Tumor Microenvironment and Reduced Expression of UFL1 Involved in PD-L1/PD-1 Pathway. To obtain an overview of the potential connections between the UFMylation activity and tumor immunogenicity, we grouped the high (top 50th percentile) and low (bottom 50th percentile) UFL1 expressions (FPKM) across 33 cancer types from The Cancer Genome Atlas (TCGA) and calculated the corresponding enrichment scores of infiltrated immune cells for each group (55). We observed that higher expression of UFL1 (or UFM1) was closely associated with immune-active ($CD8^+$ T cells, $CD4^+$ T helper cells, T-effect cells, and T-central memory cells) tumor microenvironment (Fig. 1*A*, *SI Appendix*, Fig. S1*A*, and Datasets S1 and S2). Heat map further showed the correlation between the significant abundance of tumor-infiltrated immune cells and UFL1 (or UFM1) expression (Fig. 1*B*, *SI Appendix*, Fig. S1*B*, and Datasets S1 and S2). Gene ontology (GO) analysis showed that the knockdown of UFL1 (or UFM1) expression was positively correlated with genes in immunology pathways (Fig. 1*C* and *SI Appendix*, Fig. S1*C*). Notably, the knockout of UFL1 positively correlated with the PD-L1 expression and PD-1 checkpoint pathway (Fig. 1*C*). We further found that high-level expression of UFL1 and DDRGK1 protein was positively correlated with the responders of melanoma patients with anti-PD1 therapy from a public database (56) (Fig. 1 *D* and *E* and Dataset S3). These data together suggest that UFL1 expression was closely correlated with immune-active tumor microenvironment and response of PD-1 therapy, providing a connection between UFMylation and tumor microenvironment.

Identification of PD-L1 as a Target for UFMylation. A growing number of evidence showed that UFMylation, similar to ubiquitin and ubiquitin-like protein modifications, contributes to functional regulation of substrates and thus regulates a range of biological processes (2, 5). To investigate whether PD-L1 is a target of the UFMylation modification, we first analyzed the physical interaction between UFL1 and PD-L1 and identified the binding proteins of UFL1 within PD-L1 highly expressed human cell line MDA-MB-231 through mass spectrometry analysis. Notably, PD-L1 was found as a partner of UFL1 with nine and seven unique peptides from mass spectrometry analysis of endogenous and exogenous UFL1-binding partners, respectively (Fig. 2*A*, *SI Appendix*, Fig. S2 *A* and *B*, and Datasets S4 and S5). Reciprocal immunoprecipitation analysis further confirmed that UFL1 and PD-L1 were capable of binding with each other (Fig. 2 *B* and *C*). Moreover, we found that PD-L1 can interact with other UFMylation components DDRGK1 and UFSP2, further suggesting that PD-L1 may have potential biological interactions with the UFMylation complex (Fig. 2*B*). Importantly, GST-pull-down assay showed that UFL1 directly binds with PD-L1 in vitro (Fig. 2*D*), further suggesting that PD-L1 could be a bona fide partner of UFL1. Given that UFMylation is a ubiquitin-like posttranslational modification, we are curious whether PD-L1 is a substrate of UFMylation. We first transiently coexpressed FLAG-tagged PD-L1 with HA-tagged UFMylation components UBA5, UFC1, UFL1, DDRGK1, and UFM1 in HEK293T cells as described previously (57), and the results showed that exogenous PD-L1 can be covalently conjugated by both the wild-type ($UFM1^{WT}$) and active UFM1 ($UFM1^{\Delta C2}$), but not the defective UFM1 ($UFM1^{\Delta C3}$) (Fig. 2*E*). Concordantly, we further found that endogenous PD-L1 in MDA-MB-231 cells can be UFMylated by UFM1 (*SI Appendix*, Fig. S2*C*). Likewise, we further observed that endogenous PD-L1 was identified from the His-UFM1 affinity captures in MDA-MB-231 cell (Dataset S6).

To identify which lysine residues (K) were involved in the covalent modification by UFM1 on PD-L1, we constructed a total of 19 individual mutants (lysine to arginine) and Lys less mutant ($PD\text{-}L1^{MT}$). We found that K75R, K89R, K105R, K162R, K280R, and K281R mutants significantly decreased the UFMylation of PD-L1. Notably, K89R and K162R represented the least modification of UFMylation of PD-L1 (*SI Appendix*, Fig. S2*D*). Those data indicate that the UFMylation sites of PD-L1 reside in these Lys residues. Importantly, we further detected that K89 and K162 could be covalently modified by UFM1 through mass spectrometry analysis (Fig. 2 *F* and *G*, *SI Appendix*, Fig. S2 *F* and *G*, and Dataset S7). To further explore which Lys residues were maximally required for the UFMylation of PD-L1, we constructed Lys to Arg mutations in various combinations, including $PD\text{-}L1^{2KR}$ (K89R+K162R), $PD\text{-}L1^{3KR}$ (K89R+K162R+K75R), $PD\text{-}L1^{4KR}$ (K89R+K162R +K75R+K105R), $PD\text{-}L1^{5KR}$ (K89R+K162R+K75R+K105R+K280R), and $PD\text{-}L1^{6KR}$ (K89R+K162R+K75R+K105R+K280R+K281R) and found that $PD\text{-}L1^{6KR}$ was the minimum UFMylated by UFM1 system (Fig. 2*H*), similar to the negative control of $PD\text{-}L1^{MT}$, suggesting that all the six Lys residues are required for UFMylation of PD-L1. However, this does not rule out the possibility that other Lys residues may be modified under certain physiological or pathological conditions in response to intrinsic and extrinsic stresses.

Similar to ubiquitin, the C-terminal conserved glycine residue was not only essential for UFM1-mediated conjugation on targets, but also crucial for forming a di-UFM1 or poly-UFM1 chains

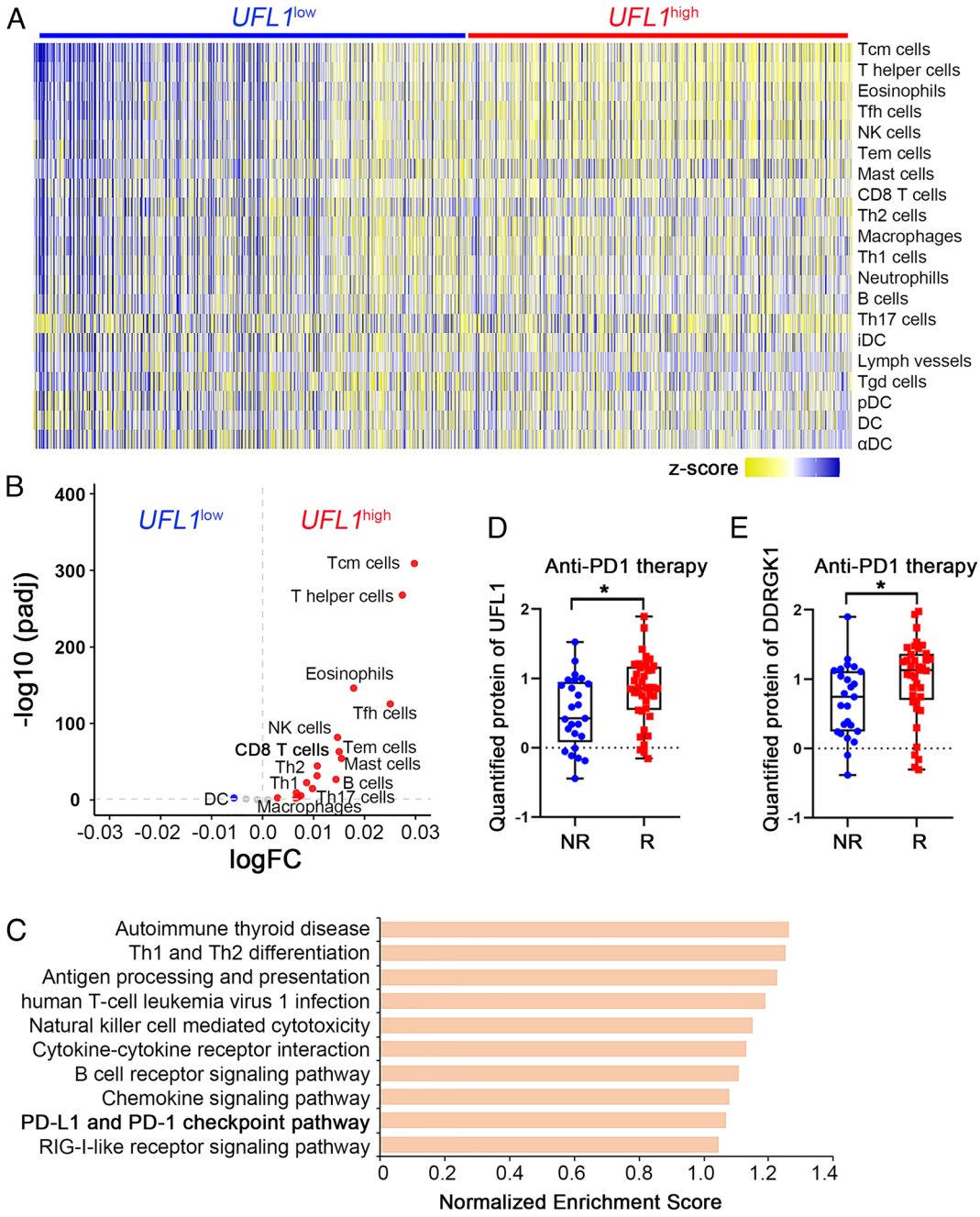

Fig. 1. High expression of UFL1 was associated with immune-active tumor microenvironment and reduced expression of UFL1 involved in PD-L1/PD-1 pathway. Scatter plot (*A*) and heat map (*B*) show differences in signatures of immune cells in UFL1^{high} and UFL1^{low} tumors, respectively, across TCGA using ssGSEA (n = 5,000 tumors for each group, pdaj < 0.05). Highly represented immune cells in high-expression tumors are shown on the *Right*, while those in low-expression tumors are shown on the *Left*. ssGSEA, single-sample gene set enrichment analysis. FC, fold change. pdaj, the adjusted *P* values. Tem: effector memory T cells, Tcm: central memory T cells, Treg: regulatory T cells, MDSC: myeloid-derived suppressor cells, TFH: follicular helper T cells, DC: dendritic cells, NK cells: natural killer cells, Tgd: gamma delta T cells, pDC: plasmacytoid DCs, Th1: T helper 1 cells; Th2: T helper 2 cells; Th17: T helper 17 cells. (*C*) GO analysis of up-regulated genes in immune [log2 (FC-KD/Ctrl)>1] and false discovery rate (FDR < 0.25) in sgUFL1 compared with control MDA-MB-231. The protein levels of UFL1 (*D*) and DDRGK1 (*E*) in tumors from melanoma patients with response (n = 40) and nonresponse (n = 25) of anti-PD1 therapy. Statistical analysis was performed using an unpaired two-sided Student's *t* test.

(5). To identify the Lys residues that are involved in the formation of di-UFM1 chains on PD-L1, all the six Lys residues on UFM1, except one of them, were substituted with Arg, and Lys less mutant (UFM1^{MT}) was used as a negative control. We found that K69 is a key Lys residue responsible for the di-UFMylation of PD-L1, which is similar to the patterns of UFMylated PD-L1 by UFM1^{WT} and active UFM1$^{\Delta C2}$. By contrast, K3, K7, K19, K34, and K41, similar to the Lys less (MT) mutant, showed very weak modification of UFMylation (*SI Appendix*, Fig. S2*E*).

UFSP2 is the primary "de-UFMylation" enzyme in human cells (4, 5, 18). Therefore, we investigated whether UFSP2 is responsible for removing UFM1 from the UFMylated PD-L1 by cotransiently overexpressing HA-UFSP2 and UFMylation components in HEK293T cells. We observed that UFSP2 could significantly diminish the conjugation of UFM1 on PD-L1 (*SI Appendix*, Fig. S2*H*). Considering that PD-L1 could interact with UFSP2 (Fig. 2*B*), those data suggest that UFSP2 acts as a de-UFMylation enzyme for PD-L1 through direct physical interaction.

A

Protein names	Gene names	Peptides	Unique peptides
E3 UFM1-protein ligase 1	UFL1	52	52
CDK5 regulatory subunit-associated protein 3	CDK5RAP3	26	26
E3 ubiquitin-protein ligase TRIM21	TRIM21	26	26
Heat shock cognate 71 kDa protein	HSPA8	20	14
DDRGK domain-containing protein 1	DDRGK1	14	14
X-ray repair cross-complementing protein 6	XRCC6	11	11
Programmed cell death 1 ligand 1	**CD274**	**7**	**7**
Ubiquitin-fold modifier 1	UFM1	5	5
Ubiquitin-fold modifier-conjugating enzyme 1	UFC1	5	5

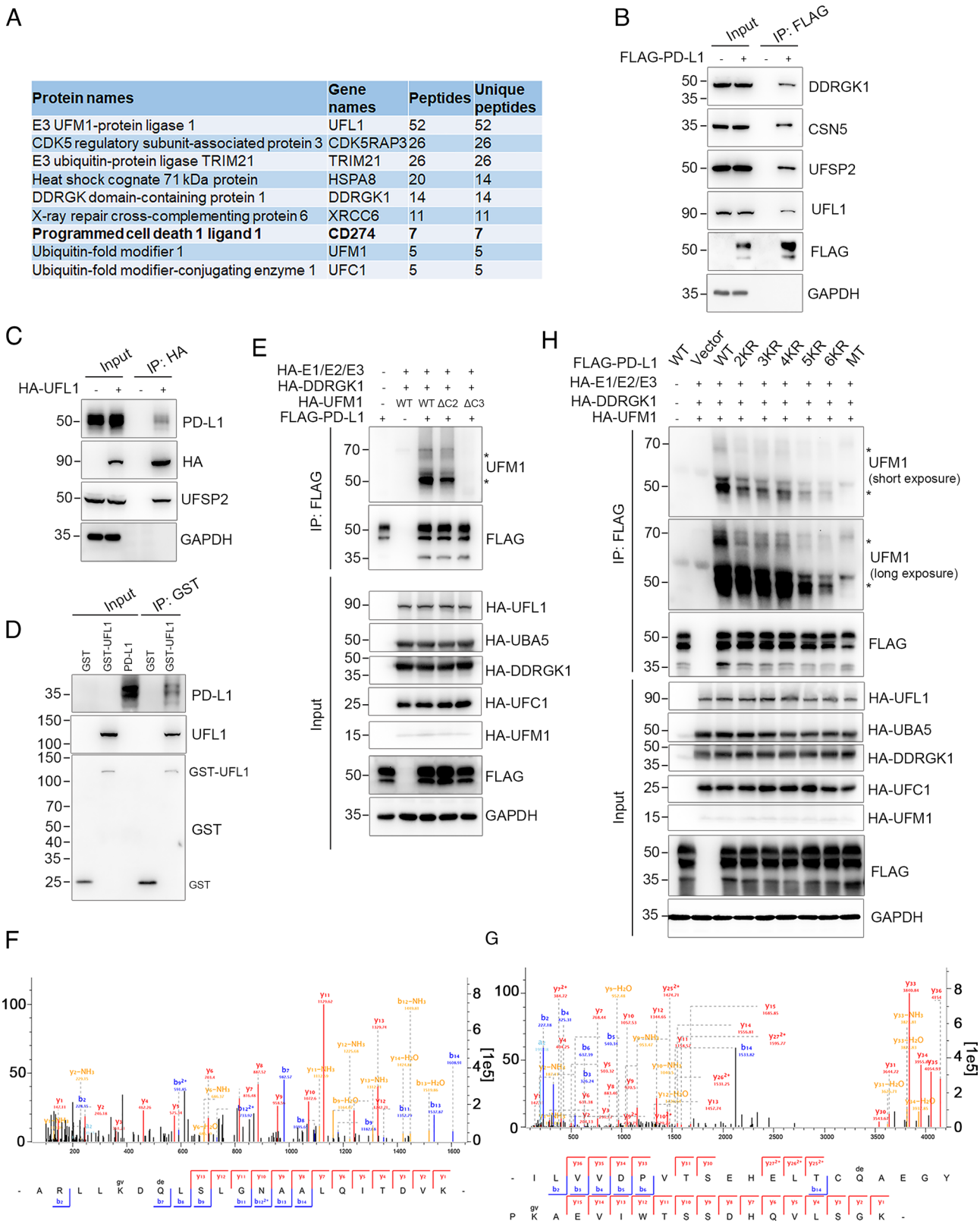

Fig. 2. Identification of PD-L1 as a target for UFMylation. (*A*) Mass spectrometry analysis identified PD-L1 as a partner of UFL1. UFL1 was immunoprecipitated from cell lysates of MDA-MB-231 cells expressing HA-UFL1, with HA-vector as a control. The immunoprecipitates were subjected to mass spectrometry analysis. Table. 1 shows some of the UFL1 binding partners which have more than five unique peptides identified from our mass spectrometry. Cell lysates were prepared from MDA-MB-231 and subjected to immunoprecipitation with anti-FLAG (*B*) or anti-HA (*C*) antibody followed by western blot analysis of the mutual interactions between UFL1, PD-L1, DDRGK1, and UFSP2. DDRGK1 and CSN5 were chosen as positive controls for UFL1 and PD-L1 binding, respectively. (*D*) Recombinant human His-tagged PD-L1 protein was incubated with GST or GST-UFL1 followed by GST pull-down assay with glutathione-Sepharose and immunoblot with indicated antibodies. (*E*) Assay for detecting the UFMylation of exogenous PD-L1. HEK293T cells were transfected with UFMylation components and FLAG-PD-L1 followed by immunoprecipitation with anti-FLAG antibody and immunoblot with anti-UFM1 antibody. UFM1ΔC2 and UFM1ΔC3 were chosen as active and defective UFM1, respectively. (*F* and *G*) Identification of lysine residues of PD-L1 modified by UFM1 through mass spectrometry. FLAG was immunoprecipitated from cell lysates of HEK293T cells expressing UFMylation components and FLAG-PD-L1, followed by mass spectrometry analysis. (*H*) UFMylation assays of wild-type PD-L1 and its mutants (K to R) in HEK293T cells expressing UFMylation components. *stands for the bands of the UFMylated PD-L1.

Moreover, to find out which lysine residues were undertaken in the covalent modification on murine PD-L1 by UFM1 modification system, we constructed a total of thirteen individual mutants (lysine to arginine) and Lys less mutant (mPD-L1^{MT}) of mPD-L1. We observed that K75R, K89R, K105R, K271R, and K280R significantly decreased the UFMylation of mPD-L1 (*SI Appendix*, Fig. S3*A*). Meanwhile, K94R slightly reduced the UFMylation of mPD-L1. Therefore, we finally selected and generated a defective UFMylation of mPD-L1^{5KR} (including K75R, K89R, K105R, K271R, and K280R). UFMylation assay further showed that mPD-L1^{5KR} significantly decreased the covalent binding of UFM1 (*SI Appendix*, Fig. S3*B*) compared with the mPD-L1^{WT}, suggesting that UFMylation sites on mPD-L1 mainly within the five Lys residues of K75, K89, K105, K271, and K280. Furthermore, we aligned the homology of lysine residues of PD-L1 of human and murine and observed that five Lysine residues are consistent with PD-L1^{6KR} and mPD-L1^{5KR}, further suggesting that those Lysine residues are crucial for modification of PD-L1 by UFM1 (*SI Appendix*, Fig. S3*C*). Importantly, mass spectrometry analysis further supported that endogenous mPD-L1 can be modified by endogenous UFM1 (*SI Appendix*, Fig. S3 *D–F*).

UFMylation of PD-L1 Promotes Its Proteasome-Mediated Degradation of PD-L1. To investigate the biological functional regulation of PD-L1 by UFMylation in cells, we depleted UFL1 or UFM1 in human cancer cell lines of MDA-MB-231, WM989, and HLF by two specific sgRNAs for UFL1 and UFM1 and found that knockout UFL1 or UFM1 significantly promoted accumulation of PD-L1 protein (Fig. 3*A* and *SI Appendix*, Fig. S4*A*). Besides, we observed that the knockdown of *Ufl1* or *Ufm1* in murine cancer cell lines MC38, B16F10, and Hepa1-6 by specific small interfering RNAs (siRNAs) significantly increased the total mPD-L1 proteins (*SI Appendix*, Fig. S4 *B* and *C*). Furthermore, exogenous expression of human UFL1-sgRNA–resistant *UFL1* cDNA in CRISPR–Cas9-mediated *UFL1* knockout cells restored the total level of PD-L1 protein in MDA-MB-231 (Fig. 3*B*), suggesting that UFL1 functions as a real regulator of PD-L1.

To further investigate whether UFL1 regulates the stability of PD-L1 in vivo, we generated the liver conditional knockout mice ($Ufl1^{fl/fl}Alb^{Cre}$) and found that the total mPD-L1 protein level was up-regulated in *Ufl1*-deprived liver tissue (Fig. 3 *C* and *D*). Meanwhile, we further observed that $Ufl1^{fl/fl}Alb^{Cre}$ mice induced a remarkably liver cancer gene signature (*SI Appendix*, Fig. S4*G*), which further suggests that *Ufl1* deprivation contributed to pathological conditions including cancer. It is worth mentioning that global UFMylated proteins were down-regulated in both UFL1 knockout MDA-MB-231 cells (*SI Appendix*, Fig. S4*D*) and $Ufl1^{fl/fl}Alb^{Cre}$ tissues (*SI Appendix*, Fig. S4 *E* and *F*), which suggested that UFL1 (or *Ufl1*) regulates the stability of PD-L1 were associated with the functional involvement of UFMylation activity. Flow cytometry analysis further confirmed that UFL1 knockout enhanced the cell surface location of PD-L1 in MDA-MB-231 and WM989 cells (Fig. 3*E*). Notably, knockout UFL1 significantly increased the cell-surface PD-L1, but not the expression of PD-L1 mRNA in the presence of IFNγ, which further suggests that UFMylation regulated PD-L1 in a manner of posttranslational modification (Fig. 3*F*). Moreover, immunofluorescence results visually showed that the knockout of UFL1 enhanced the cell-surface PD-L1 in MDA-MB-231 cells (Fig. 3 *G* and *H*). Together, our data suggest that dysUFMylation stabilizes the PD-L1 protein in both levels of cells and in vivo. We examined the PD-L1 stability in MDA-MB-231 and HLF cells treated with cycloheximide (CHX) and found that PD-L1 stability was significantly increased after depletion of UFL1 (Fig. 3 *I* and *J* and *SI Appendix*, Fig. S5 *A* and *B*). Concordantly, we observed that human PD-L1^{6KR} and murine PD-L1^{5KR} were increased in endogenous PD-L1 knocked-out human and murine cancer cell lines (termed MDA-MB-231^{KO}, HLF^{KO}, Hepa1-6^{KO}, and MC38^{KO}) treated with CHX compared with the corresponding controls (Fig. 3 *K* and *L* and *SI Appendix*, Fig. S5 *C–H*). These data further supported that dysUFMylation of PD-L1 stabilizes PD-L1 protein. Given that ubiquitination, glycosylation, and lysosome-mediated degradation are crucial ways for regulating the stability of PD-L1 (44, 45, 58–60), we are curious whether the mechanisms underlining the UFMylation regulating the stability of PD-L1 are related to those ways. We treated cells with the inhibitors of the proteasome (MG132) and lysosome (HCQ) and found that cells of MDA-MB-231-sg*UFL1*, MDA-MB-231^{KO}-PD-L1^{6KR}, and MC38^{KO}-mPD-L1^{5KR} were insensitive to MG132 treatment compared with their controls (Fig. 3 *M* and *N* and *SI Appendix*, Fig. S5*I*), which suggests that the dysregulation of UFMylation may antagonize the proteasome-mediated degradation of PD-L1. To further clarify the potential regulatory relationship between UFMylation and ubiquitination, we transiently coexpressed FLAG-tagged PD-L1^{WT} (or FLAG-tagged PD-L1^{6KR}) with UFMylation components and His-tag Ub in HEK293T cells, then treated with MG132, and found that the increased activity of UFMylation promoted the ubiquitination of PD-L1^{WT} compared with PD-L1^{6KR}, which further supported that dysUFMylation maintained the stability of PD-L1 by antagonizing its ubiquitination (Fig. 3*O*). Moreover, we also observed that there is no significant difference of total glycoprotein between UFL1 knocked-out and control cells (*SI Appendix*, Fig. S5 *J* and *K*), suggesting that dysUFMylation promoted the stability of PD-L1 which is independent of the modification of glycosylation. Together, these data suggest that dysregulation of UFMylation could diminish the ubiquitination of PD-L1, thereby stabilizing PD-L1 by counteracting its proteasome-mediated degradation.

DysUFMylated PD-L1 Diminished CD8$^+$ T Cell-Mediated Tumor Immunity. Cancer cells exploit the PD-L1/PD-1 pathway to evade CD8$^+$ T cell-mediated immune surveillance (43, 61). To investigate whether dysUFMylation of PD-L1 affects the PD-1–binding and CD8$^+$ T cell-mediated cytotoxicity, recombinant human PD-1 Fc chimera protein was incubated with MDA-MB-231 sg*UFL1* and control cells. Flow cytometry and immunofluorescence assays showed that disruption of *UFL1* significantly increased the binding of PD-1 to tumor cell surface (Fig. 4 *A* and *B*). Consistently, coculture assay showed that deletion of UFL1 decreased the sensitivity of tumor cells to activated T cell killing (Fig. 4*C*). Giemsa staining further showed that disruption of UFL1 diminished the sensitivity of tumor cells from CD8$^+$ T cell killing, and promoted the survival of cancer cells with increased PD-L1 and decreased expression of caspase-3, respectlively (Fig. 4 *D* and *E*). Immunoblotting further revealed the decreased granzyme B (GZMB), phospho-Akt, and phospho-ERK in the activated human peripheral blood mononuclear cells cocultured with UFL1 knocked-out tumor cells (Fig. 4*E*). In contrast, we found that the deletion of UFL1 did not affect the growth of tumor cells when tumor cells cultured alone (*SI Appendix*, Fig. S6*A*). These data suggested that UFL1 is involved in T cell-mediated immune response in tumor microenvironment.

To further investigate the role of UFMylation on PD-L1 in vivo, we first constructed endogenous mPD-L1 knocked-out MC38 cells by specific sgRNAs and substituted with sgRNA-resistant cDNA of mPD-L1^{WT} and mPD-L1^{5KR} cell lines (termed MC38^{KO}-mPD-L1^{WT} and MC38^{KO}-mPD-L1^{5KR}, respectively). Similar to the previous results of PD-L1^{6KR} in human cancer cell

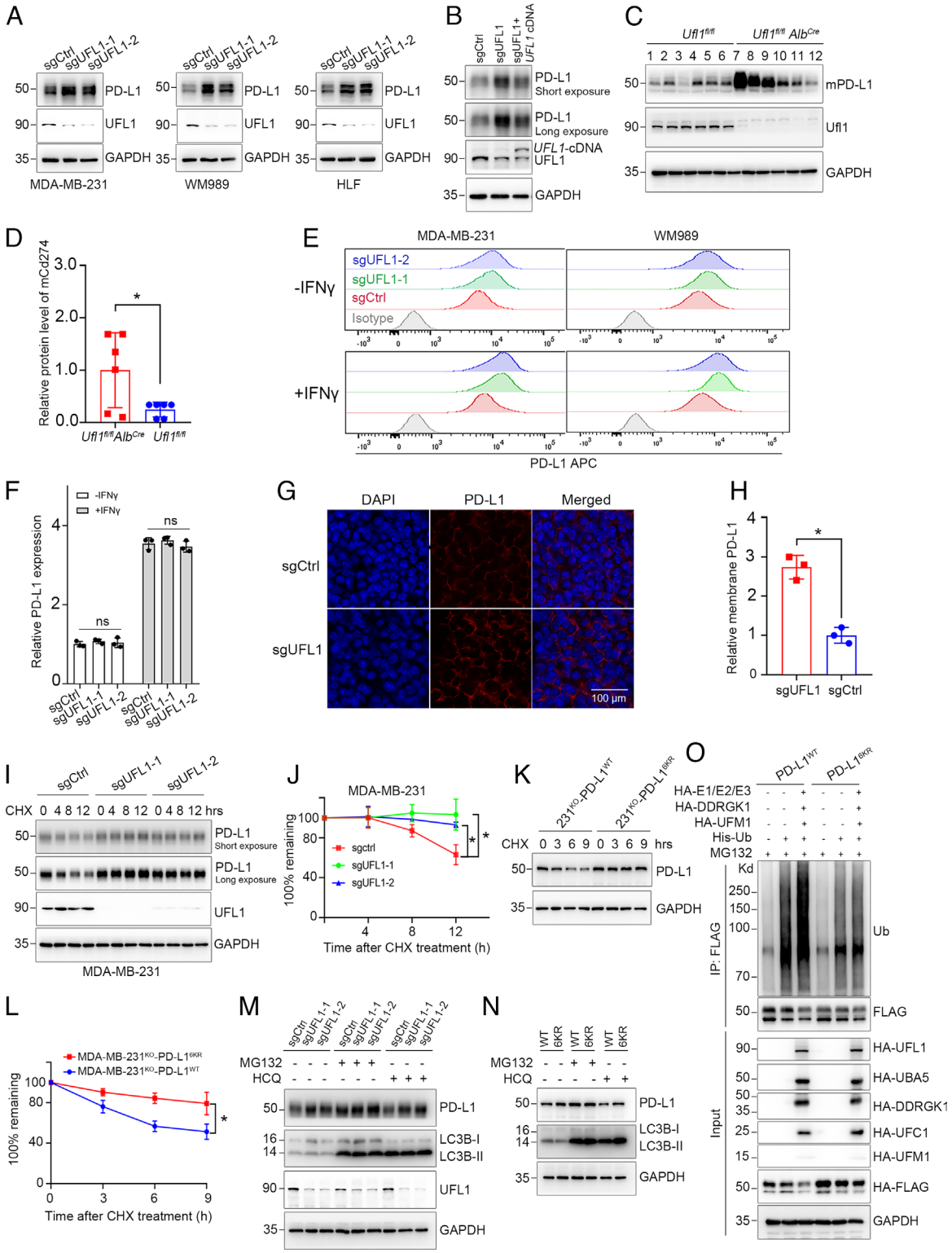

Fig. 3. UFMylation destabilized PD-L1 by promoting its proteasome-mediated degradation. (*A*) Western blot analysis of PD-L1 protein in MDA-MB-231 cells with UFL1 knockdown by specific sgRNAs. (*B*) Western blot analysis of PD-L1 expression in UFL1 knockout MDA-MB-231 cells in the absence or presence of UFL1 cDNA. (*C* and *D*) Immunoblot analysis of mPD-L1 expression in liver tissues from *Ufl1*$^{fl/fl}$ and *Ufl1*$^{fl/fl}$ *Alb*^{Cre} mice (n = 6). Statistical analysis was performed using an unpaired two-sided Student's *t* test. *$P < 0.05$. (*E*) Flow cytometry analysis of cell-surface PD-L1 in UFL1 knockout cells and control cells in the absence or presence of IFNγ treatment. (*F*) qPCR analysis of *PD-L1* mRNA expression in UFL1-KO MDA-MB-231 and control cells treated with IFNγ for 48 hours. (*G* and *H*) Representative sections of immunofluorescent staining of PD-L1 in UFL1 knockout versus control MDA-MB-231 cells (*G*). Quantification of the intensity of the membrane PD-L1 (*H*). (*I*) PD-L1 stability was determined by western blot in UFL1 knockout versus control MDA-MB-231 cells. Cells treated with 100 μg/mL cycloheximide (CHX) for the indicated times. (*J*) The quantification of the PD-L1 protein levels. Statistical analysis was performed using an unpaired two-sided Student's *t* test. Three biological replicates (mean, SEM). (*K* and *L*) MDA-MB-231^{KO}-PD-L1^{WT} and MDA-MB-231^{KO}-PD-L1^{6KR} were treated with 100 μg/mL cycloheximide (CHX) for the indicated times followed by immunoblot with anti-FLAG (*K*). The relative levels of PD-L1 protein were quantitated (*L*). Statistical analysis was performed using an unpaired two-sided Student's *t* test. Three biological replicates (mean, SEM). (*M*) UFL1 KO cells were treated with MG132 (20 μM) or HCQ (100 μM) for the indicated times followed by western blot with anti-PD-L1. (*N*) MDA-MB-231^{KO}-PD-L1^{WT} and MDA-MB-231^{KO}-PD-L1^{6KR} were treated with MG132 (20 μM) or HCQ (100 μM) for the indicated times followed by western blot with anti-PD-L1. (*O*) Ubiquitination of PD-L1^{WT} and PD-L1^{6KR} was analyzed by western blot in HEK293T cells expressing His-Ub alone or His-Ub and UFMylation components together.

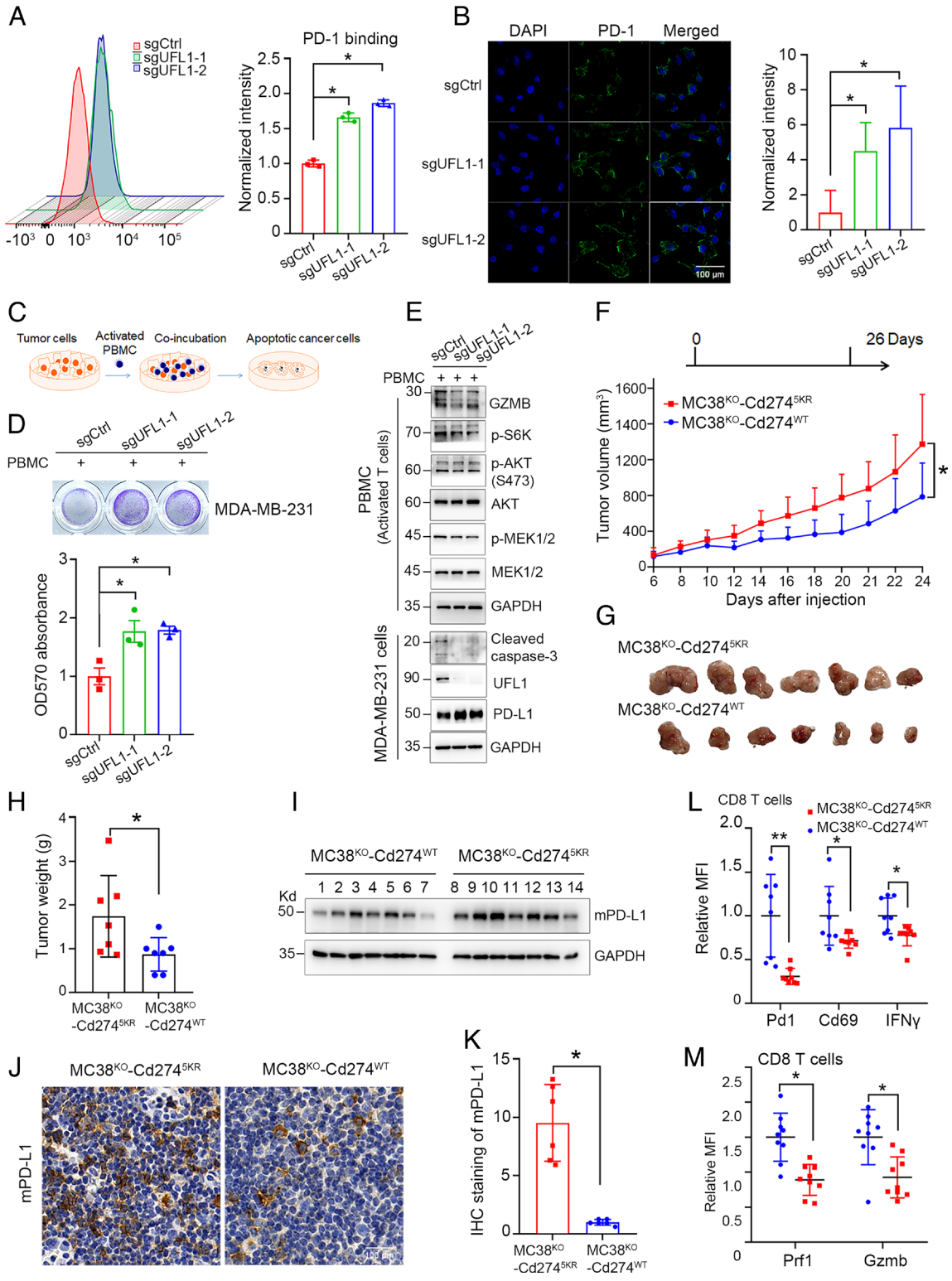

Fig. 4. Dysregulation of UFMylation stabilizes PD-L1 to promote tumor growth by interdicting the infiltration of $CD8^+$ T cells. (*A*) PD-1 binding was examined by flow cytometry in MDA-MB-231 cells with UFL1-specific or control sgRNAs. The Y axis shows the normalized mean fluorescence intensity. *P* values were calculated by two-sided Student's *t* test. (*B*) Representative sections of immunofluorescent staining of PD-1 (fused to Ig-Fc) in MDA-MB-231 cells treated by UFL1-specific sgRNAs. Quantification of the intensity of the membrane-localized PD-1. (Scale bar indicates 20 μm.) *P* values were calculated by two-sided Student's *t* test; (*C*) Schematic diagram for the experimental procedures of coculture assay. PBMC, peripheral blood mononuclear cells. T cell killing assay of MDA-MB-231 cells treated with sgRNAs for UFL1 sand control sgRNA. (*D* and *E*) Crystal violet staining of nonapoptosis MDA-MB-231 cells after cocultured with T cells for 24 h (*D*). Western blot analysis of GZMB, PRF1, MEK1/2, and p-AKT for T cells and Caspase-3 and UFL1 for MDA-MB-231 cells (*E*). (*F*) Tumor growth curves of $MC38^{KO}$-mPD-$L1^{WT}$ and $MC38^{KO}$-mPD-$L1^{5KR}$ cells in C57 BL/6J mice, respectively, and tumors were measured at the indicated times (n = 7 mice per group). *P* values were calculated 26 d after injection by two-sided Student's *t* test. (*G*) Representative pictures of tumors derived from $MC38^{KO}$-mPD-$L1^{WT}$ and $MC38^{KO}$-mPD-$L1^{5KR}$ cells. (*H*) Quantification of the tumor weight is shown. (*I*) Western blot analysis of mPD-L1 expression in tumors derived from $MC38^{KO}$-mPD-$L1^{WT}$ and $MC38^{KO}$-mPD-$L1^{5KR}$ cells. (*J* and *K*) Representative sections of immunohistochemical staining of mPD-L1 in tumors derived from $MC38^{KO}$-mPD-$L1^{WT}$ and $MC38^{KO}$-mPD-$L1^{5KR}$ cells (*J*). Quantification of the PD-L1 expression in tumors is shown (*K*). (*L* and *M*) Flow cytometry analysis of the activation markers (Pd-1, Cd69, and IFNγ) (*L*) and cytotoxicity markers (Gzmb, Prf1) (*M*) of $CD8^+$ T cell population from the isolated tumor-infiltrating lymphocytes. The graphs show means ± SD and *P* values were calculated by two-sided Student's *t* test; $^{**}P < 0.01$. $^{*}P < 0.05$.

lines MDA-MB-231 and HLF, mPD-L1^{5KR} significantly enriched the mPD-L1 protein with no changes in cell growth, cell cycle, and DNA replication compared with controls (*SI Appendix*, Fig. S6 *B* and *C*). We further subcutaneously injected C57BL/6J mice with MC38^{KO}-mPD-L1^{WT} and MC38^{KO}-mPD-L1^{5KR}. Consistent with the results from the coculture assay, mPD-L1^{5KR} significantly promoted the tumor growth with higher expression of mPD-L1 compared with mPD-L1^{WT} (Fig. 4 *F*–*I* and *SI Appendix*, Fig. S6*D*). Immunohistochemistry analysis of tumor tissues revealed that mPD-L1^{5KR} promoted mPD-L1 protein accumulation and membrane distribution (Fig. 4 *J* and *K*). Meanwhile, flow cytometry evaluated the CD8$^+$ T cell response in tumor tissues and showed that mPD-L1^{5KR} not only inhibited the activation of CD8$^+$ T cells by decreased expression of Pd1, Cd69, and IFNγ, but also interdicted T cell cytotoxicity by decreased expression of Gzmb and Prf1, compared with the mPD-L1^{WT} tumors (Fig. 4 *L* and *M*). Because GZMB is largely produced by CD8$^+$ T cells and NK cells and induces tumor cell apoptosis (62), the above results suggested that dysUFMylation could impair the activities of toxic CD8$^+$ T cells and disturb the tumor immune microenvironment in dependent of PD-L1 pathway. In support to this conclusion, MC38^{KO}-mPD-L1^{WT} and MC38^{KO}-mPD-L1^{5KR} were subcutaneously injected into immune-deficient BALB/c nude mice and we found there were no difference in both tumor volumes and weights between tumors of MC38^{KO}-mPD-L1^{WT} and MC38^{KO}-mPD-L1^{5KR}, respectively (*SI Appendix*, Fig. S6 *E* and *F*), our results partially support that dysregulation of PD-L1 modification by UFM1 could play a role in subverting the CD8$^+$ T cell-mediated immune surveillance. Collectively, these results suggested that the UFMylation system plays a key role in the functional regulation of PD-1/PD-L1 pathway.

We further evaluated the effects of MC38^{KO}-mPD-L1^{WT} and MC38^{KO}-mPD-L1^{5KR} on tumor growth after anti-mPD-1 or IgG treatment. Consistent with the aforementioned results, mPD-L1^{5KR} significantly promoted tumor growth (*SI Appendix*, Fig. S6*G*). As expected, mPD-1 blockade by anti-mPD-1 antibody dramatically inhibited tumor growth of both MC38^{KO}-mPD-L1^{WT} and MC38^{KO}-mPD-L1^{5KR} (*SI Appendix*, Fig. S6 *H* and *I*). Notably, we also observed that MC38^{KO}-mPD-L1^{WT} with the lower expression of mPD-L1 showed a slower tumor growth rate and an extended survival from anti-PD1 treatment compared with the MC38^{KO}-mPD-L1^{5KR} (*SI Appendix*, Fig. S6*J*), which may relate to the fact that decreased PD-L1 coulde reduce the binding to PD-1 and thereby enhances antitumor immunity. This observation further supports that inhibition of PD-L1 could enhance an efficacy of anti-PD-1 therapy (45).

UFL1 Expression Was Decreased and Negatively Correlated with Levels of PD-L1 in Human Cancers. To investigate the patterns of UFMylation gene expression in clinical samples, we found that the expression of UFL1 was significantly decreased in liver cancer tissues compared with adjacent normal tissues (Fig. 5 *A* and *B*) and negatively correlated with PD-L1 expression through human tissue microarray (Fig. 5 *C* and *D*). In addition, we also found that UFL1 expression was reduced in patients with melanoma based on TCGA database (*SI Appendix*, Fig. S7*A*). Moreover, we found that *Ufl1* and *Ddrgk1* expression was down-regulated in chemical-induced mouse liver cancer models (*SI Appendix*, Fig. S7 *B* and *C*), which further supports that loss of *Ufl1* may induce pathological diseases. Notably, we performed Kaplan–Meier analysis and found that the low expression of *UFL1* was closely associated with poorer overall survival in both patients with liver cancer (Fig. 5*E*) and melanoma (*SI Appendix*, Fig. S7*D*). Taken together, our findings suggest that UFL1 could function as a tumor suppressor by regulating the stability of PD-L1 (Fig. 5*F*).

Compound-8, a Covalent Inhibitor of UFSP2, Promotes UFMylation Activity and Contributes to Immunotherapy with Anti-PD-1. Inhibition of UFSP2 significantly enhances the global UFMylation activity in cells and thus increases the UFMylation of substrates. Our findings above revealed that UFMylation of PD-L1 could promote the ubiquitination degradation of PD-L1. We then sought to provide in vivo proof-of-principle data to test the clinical translational potential of our findings by identifying covalent inhibitors of UFSP2. In order to screen inhibitors of UFSP2, we performed virtual screening of target molecule library with software Schrodinger (Maestro) (Fig. 6*A*). We first selected the crystal structure of 3OQC (UFSP2) as the receptor protein from PDB database and the recently published AlphaFold protein structure database. Since the substrate-binding cavity of the catalytic site (Cys294) of UFSP2 is relatively narrow, we selected covalent inhibitor molecular library for virtual screening of small-molecule inhibitors. Covalent Docking in Schrodinger software was used to evaluate the ability of various covalent inhibitor molecules to form covalent bonds with Cys294 of UFSP2 (Fig. 6*A*). According to the binding conformation and energy scoring, we finally obtained eight top-ranked candidates of inhibitors from the library of 3,000 covalent inhibitors (Fig. 6*B*). We observed that compound-8 could significantly and consistently improve the global UFMylation activity in both MDA-MB-231 and MC38 cells. Meanwhile, compound-8 decreased the expression of PD-L1 without affecting the UFSP2 protein levels (Fig. 6 *C*–*E* and *SI Appendix*, Fig. S8*A*). To investigate the specificity of compound-8 in the regulation of UFMylation activity, we treated MDA-MB-231 and MC38 cells with compound-8 at indicated concentrations and found that compound-8 dose dependently enhanced the global UFMylation proteins while decreasing the expression of PD-L1 (Fig. 6*F* and *SI Appendix*, Fig. S8*B*). Moreover, we observed that compound-8 significantly promoted the modification of PD-L1 by UFMylation in cell assay of UFMylation (Fig. 6*G*). Lastly and importantly, we observed the tumor-suppressive effect of compound-8 in the MC38 tumor mouse model. Although PD-1 blockade and compound-8 treatment showed different tumor-suppressive effects, the combination treatment yielded a better antitumor effect with no appreciable body weight loss (Fig. 6 *H*–*K*).

Discussion

Blockage of PD-1/PD-L1 pathway prevents the PD-L1 on cancer cell surface from binding with PD-1, thereby promoting T cell-mediated antitumor response (33, 53). However, the relatively low response rate of anti-PD-1/PD-L1 therapy and ICB resistance highlight the need for further improvement in therapy. Further study and improvement requires a more in-depth understanding of how PD-L1 is being regulated in tumor cells (43). Here, we revealed that UFMylation (or dysregulation of UFMylation) of PD-L1 could regulate the stability of PD-L1. On the basis of our findings, we conclude that UFL1 expression is down-regulated and closely associated with poorer overall survival rate in patients with melanoma or liver cancers. Importantly, lower expression of UFL1 positively correlated with immune-suppressive microenvironment, PD-L1 expression, and nonresponse of anti-PD1 therapy. Interestingly, the mPD-L1 expression was dramatically increased in liver tissues from *Ufl1* conditional knockout mice with induced liver cancer signature genes, which further suggests that UFL1 may function as a true tumor

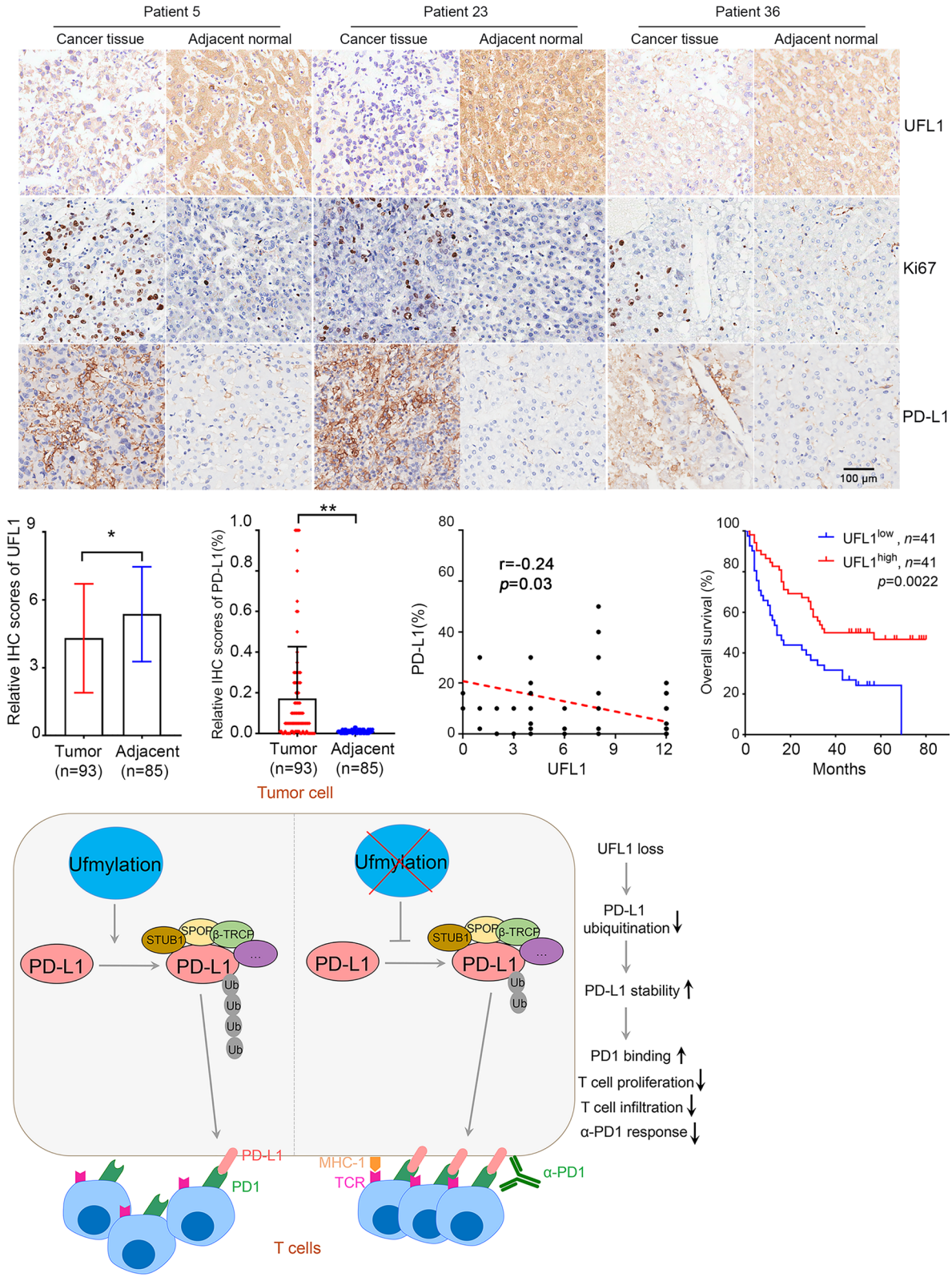

Fig. 5. UFL1 expression was decreased and negatively correlated with levels of PD-L1 in human cancers. (*A*) Representative sections of immunohistochemical staining of UFL1, PD-L1, and Ki67 in 90 pairs of human liver cancers and adjacent normal tissues in tissue array. Quantification of the relative IHC scores of UFL1 (*B*) and PD-L1 (*C*) from liver cancer (n = 93) and adjacent normal tissues (n = 85), respectively, in tissue array. Statistical analysis was performed using an unpaired two-sided Student's *t* test. **<0.01. (*D*) Correlation analysis of UFL1 expression and the levels of PD-L1 in 90 pairs of liver cancers and adjacent normal tissues (r = −0.24, *P* = 0.03). (*E*) Kaplan–Meier analysis of overall survival rate in patients with hepatocellular carcinoma according to the high- and low-level expression of UFL1 (two-sided Mantel–Cox log-rank test; n = 41). (*F*) Working model of UFMylation and dysUFMylation of PD-L1 in tumor microenvironment.

suppressor in tumorigenesis. It could be speculated that copy number loss could contribute to the decreased expression of UFL1 in various cancer types including melanoma from the genomic signatures of UFMylation family (18). However, how UFL1 expression was down-regulated and contributed to the hepatocarcinogenesis remains to be answered.

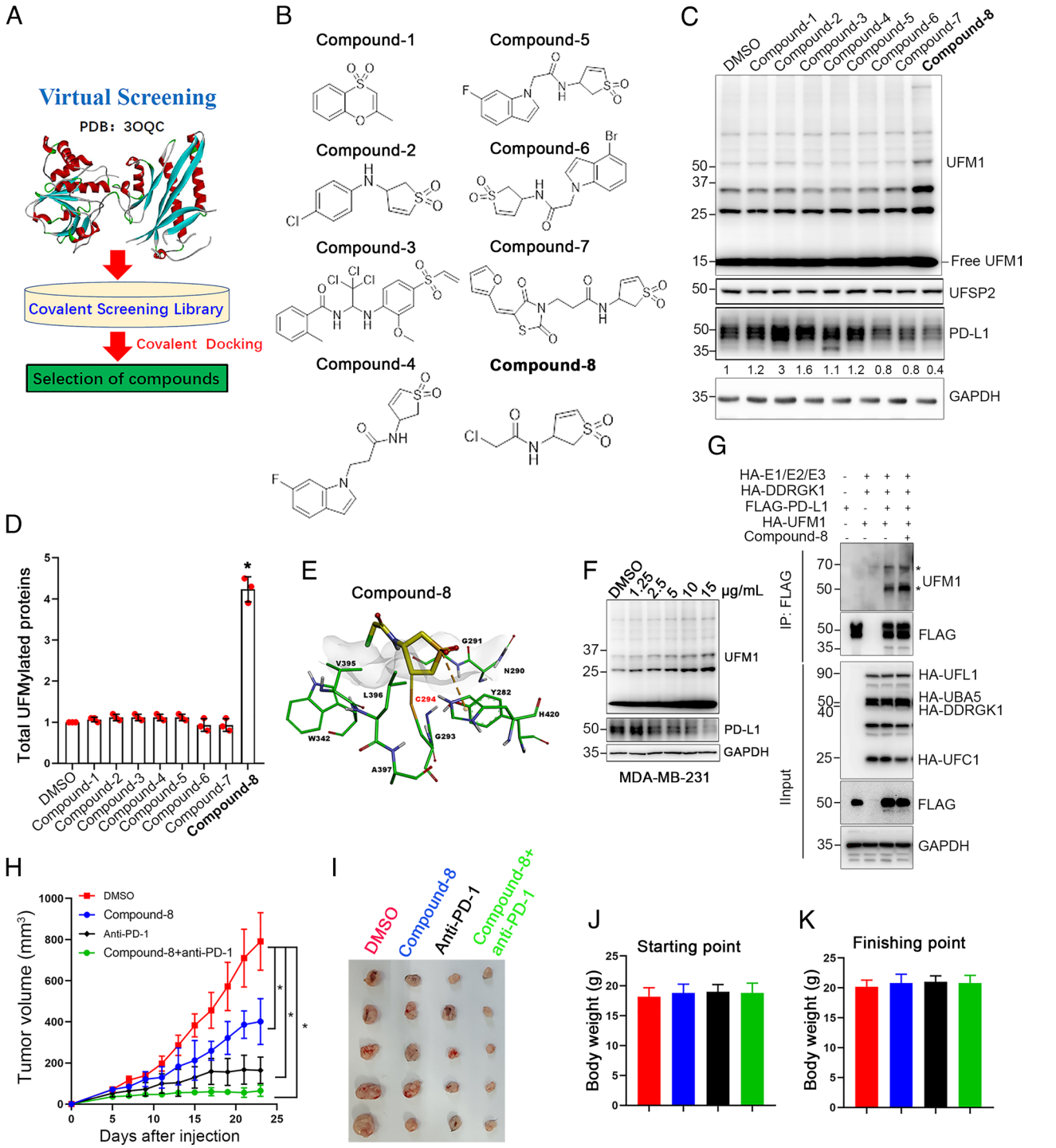

Fig. 6. Covalent inhibitor of UFSP2 promoted UFMylation activity and contributed to immunotherapy with anti-PD-1. (*A*) Working model of the virtual screening. (*B*) Structures of compounds. (*C* and *D*) The global UFMylation activity was measured by western blot in MDA-MB-231 cells treated with compounds for 48 h (*C*). Quantification of UFMylation activity is shown (*D*). (*E*) Crystal structure of UFSP2 (3OQC) in complex with compound-8. UFSP2 (green) with relevant side chains in stick representation; Compound-8 is shown in yellow. The catalytic site (Cys294) of UFSP2 is shown in red. Gray bands stand for the interaction region between UFSP2 and comppund-8. (*F*) The global UFMylation activity and endogenous PD-L1 were measured by immunoblot in MDA-MB-231 cells treated with indicated dose of compound-8 for 48 h. (*G*) Assay of UFMylation for PD-L1 in MDA-MB-231 treated with 5 μg/mL compound-8 for 48 h. *stands for the bands of the UFMylated PD-L1. (*H*) Tumor growth curves of MC38 in C57BL/6J mice with indicated treatments. (*I*) Representative pictures of tumors derived from (*H*). (*J* and *K*) Body weights of mice from (*I*). *P* values, Student's *t* test. *$P < 0.05$; **$P < 0.01$.

Furthermore, using the assays of reciprocal coimmunoprecipitation, GST pull down, exogenous and endogenous UFMylation detection, and identification of modification site, we demonstrated that PD-L1 could be a bona fide substrate of UFMylation through direct physical interaction. Recent studies have revealed that several targets (e.g. MRE11/H4, DDRGK1, p53, and RPL26, et al.) can be modified by UFMylation in response to DNA damage, ER stress, and abnormal stalled ribosome, respectively. However, there is little information on how UFMylation has taken place and has been coordinated. Thus, the temporal and spatial

regulation of Lysine residues on PD-L1 under a wide variety of intrinsic and extrinsic stresses merits future investigation to clirify the relationship between ubiquitination, acetylation, glycosylation, phosphorylation, and palmitoylation (42, 51). Importantly, we further found that dysUFMylation, such as knockout UFL1 or defective UFMylation of PD-L1, promoted the stability of PD-L1 and its membrane location through antagonizing the proteasome-mediated degradation of PD-L1 across a range of both human and murine cancer cell types. To provided more information to support the connection between PD-L1 UFMylation and ubiquitination, we identified that nine lysine residues on PD-L1 that can be covalently binds ubiquitin after batches of mass spectrometry data analysis, including K46, K75, K89, K105, K129, K136, K178, K189, and K271. Using ubiquitin assay, we further observed that K46, K89, K129, K136, K162, and K280 are important for ubiquitin-mediated PD-L1 degradation (*SI Appendix*, Fig. S9 *A* and *B* and Dataset S8). It is worth mentioning that we observed that K89, K162, and K280 can also be conjugated to UFM1 modification. Therefore, we speculated that K46, K129, and K136 may function as primary and specific Lys residues for ubiquitin-mediated PD-L1 degradation. Moreover, our preliminary data suggested that ubiquitin is a potential target of UFMylation. There is a possibility that PD-L1 could be modified by the UFM1–ubiquitin mixed chains. Furthermore, mass spectrometry analysis was used to identify the potential E3 ligases of PD-L1 in MDA-MB-231 cells with or without UFL1 expression, and we found that several potential E3 ligases (e.g., ITCH, HIP1R, OTUB1, USP16, RNF34, RNF185, TRIP12, UBR1, and UBR3) may involve in the ubiquitination of UFMylated PD-L1 (Dataset S9). The detailed mechanisms by which UFMylation promoted the proteasome-mediated degradation of PD-L1 need to be uncovered.

The defective UFMylated PD-L1 significantly promoted tumor growth in syngeneic mouse cancer model compared with controls, but it is not observed in cancer cells cultured alone that lack of immune microenvironment, suggesting dysregulation of PD-L1 by UFMylation accelerates the tumor growth was dependent on tumor immune microenvironment. As expected, we found that dysUFMylated PD-L1 promoted the binding of PD-1 and thereby decreased the activation and proliferation of $CD8^+$ T cells. Our data showed that dysUFMylation of PD-L1 increases the membrane localization of PD-L1 and its binding ability to PD-1, which may affect the response to immunotherapy with anti-PD1/PD-L1 antibody. In line with this hypothesis, we found that $mPD\text{-}L1^{5KR}$ promoted tumor growth and reduced the overall survival of tumor-bearing mice, suggesting its insensitivity to anti-PD1 treatment compared with $mPD\text{-}L1^{WT}$. It has been reported that the reduced expression of PD-L1 by gefitinib, inhibitor of EGFR, enhanced the efficacy of anti-PD1 therapy (45). Thus, we speculate that increased UFMylation activity may promote PD-1 therapy through effectively degrading PD-L1, which could partially explain why higher expression of UFL1/UFM1 positively correlates with the response of anti-PD-1 therapy. In support of our deduction, we used virtual screening and identified that a compound-8, a covalent inhibitor of UFSP2, could significantly promote UFMylation activity and contribute to anti-PD-1 therapy, suggesting that UFMylation system is a potential therapeutic target for cancer.

Materials and Methods

SI Appendix, Supporting Materials and Methods provides information on library preparation for transcriptome sequencing, GO (gene ontology) analysis, antibodies and reagents, immunoprecipitation, GST pulldown, tissue microarray, immunohistochemistry, UFMylation site identification by mass spectrometry analysis, denaturing His-tag affinity capture, mass spectrometry and data analysis, PD-L1 ubiquitination assay, immunofluorescence, and animal experiments.

Cells, Transfection, and Plasmids. HEK293T, MDA-MB-231, WM989, HLF, MC38, B16F10, and Hepa1-6 were maintained in Dulbecco's Modified Eagle Medium (Biological Industries) with 10% fetal bovine serum (FBS; HyClone), 100 U/mL penicillin, and 100 μg/mL streptomycin. U2OS cells were maintained in McCoy's 5A medium (Biological Industries) with 10% FBS, 100 U/mL penicillin, and 100 μg/mL streptomycin. All the cell lines were purchased from ATCC and mycoplasma is negative of each cell line.

To transiently express plasmids in HEK293T cells, PEI transfection solution was used (57). For transfection of siRNAs in different cancer cell lines, Lipofectamine 3000 (Invitrogen) was used, according to the manufacturer's instructions. The siRNAs used in this study are described in Dataset S10. The sense sequences of siRNAs were as follows: *Ufl1*-1: GUGGUCGAGUAAACAUUGUTT; *Ufl1*-2: GCAGCCAUUACAAGUGAUATT; *Ufm1*-1: GCAGCUACAAGUGCGAUUATT; *Ufm1*-2: GCUCAGAACUGAGAAUCAUTT. The siRNAs were purchased from GenePharma. All plasmids used in this study are described in Dataset S11.

UFMylation Detection. An optimized protocol to detect protein UFMylation was performed as previously described (57). For exogenous PD-L1 UFMylation, we transiently transfected the expression plasmids of UFMylation components (UBA5, UFC1, UFL1, DDRGK1, and UFM1) and the Flag-tagged PD-L1 into HEK293T cells using PEI solution buffer, followed by immunoprecipitation with anti-Flag beads and immunoblotting to detect the UFMylated protein with the UFM1 antibody. For endogenous PD-L1 UFMylation in MDA-MB-231 cells, cells were lysed by boiling in lysis buffer [150 mM Tris-HCl (pH 8), 5% SDS, and 30% glycerol]. Cell lysates were diluted 20-fold with buffer A (50 mM Tris-HCl pH 8.0, 150 mM NaCl, 10 mM imidazole, 1% NP-40, 2 mM NEM, and protease inhibitor cocktail). Supernatants were incubated with anti-PD-L1 antibody overnight, followed by incubating Protein-A/G Plus beads (Santa Cruz) for 2 h at 4 °C. After washing with NP-40 buffer for several times, the immunoprecipitates were analyzed by western blotting with anti-UFM1 antibody. For the detection of UFMylated PD-L1, mouse anti-rabbit IgG light chain-specific (Abbkine, A25022) antibody was used.

PD-L1/PD-1 Binding Assay. The PD-1 binding assay was performed as previously described (59). Briefly, for flow cytometry assay, UFL1 knockout and control MDA-MB-231 cells were seeded into gelatin-coated 6-well plates and allowed to reach 60% confluence, followed by trypsin digestion and washing with 1×phosphate-buffered saline (PBS). Cells were incubated with 5 μg/mL recombinant human PD-1 FC chimera protein (1:100) (R&D Systems; 1086-PD-050,) at room temperature for 1 h. The cells were washed with PBS buffer three times before incubating with anti-human IgG (H+L) Alexa Fluor 488 dye conjugated antibody (Invitrogen; A-11013; dilution; 1: 400) for 30 min at room temperature. After washing with PBS buffer, the cells were suspended in staining buffer. The cells were analyzed by flow cytometry using BD LSR Fortessa and the data were analyzed using FlowJo.

Tumor Cell Killing Assay. The protocol was performed as previously described (59). UFL1 knockout and control MDA-MB-231 cells were seeded in gelatin-coated 12-well plates at a density of 1×10^5 cell/well. Human PBMC (peripheral blood mononuclear cells) cells were seeded at a density of 1×10^6 cell/well and activated with 100 ng/mL CD3 antibody (BioLegend; 317303), 100 ng/mL CD28 antibody (BioLegend; 302913), and 10 ng/mL IL2 (BioLegend; 589102) for 24 h in 96-well round-bottomed plate, followed by transferring the activated PBMCs to the cancer cells at a ratio of 10:1 and performing coculture for 24 h. Then, PBMCs were collected and subjected to western blot. Survival analysis of cancer cells was performed by crystal violet staining and immunoblotting.

Data, Materials, and Software Availability. Raw RNA-seq data have been deposited in NCBI Gene Expression Omnibus (GSE217684). All study data are included in the article and/or *SI Appendix*.

ACKNOWLEDGMENTS. We appreciate the facilities of flow cytometry and biochemistry provided by the School of Basic Medicine, Hangzhou Normal University,

and Animal Facilities of Shenzhen Bay Laboratory for assistance with animal care. We are grateful to Dr. Jun Wei (Institute of Hematology, Chinese Academy of Medical Sciences), Dr. Hu Wang (School of Basic Medicine, Hangzhou Normal University), Dr. Jian Cao (Rutgers Cancer Institute of New Jersey, The State University of New Jersey), and Dr. Chun-yang Bao (Dana-Farber Cancer Institute, Harvard University) for insightful discussions. Dr. Shuo Mou (OrigiMed Inc) provided help in TCGA bioinformatics analysis. We thank Novogene (Beijing, China) and Micrometer Biotech Company (Hangzhou, China) for RNA sequencing and performing the LC-MS/MS analysis, respectively. This work was supported by grants from the excellence program of Hangzhou Normal University (4125C5021920462 to J.Z.), entrepreneurship program for high-level overseas returnees of Hangzhou (4125F5062100611 to J.Z.)and Key Project of Shenzhen Bay Laboratory (S201101004 to Y.Z.).

Author affiliations: [a]School of Basic Medicine, Hangzhou Normal University, Hangzhou 311121, China; [b]School of Pharmacy, Hangzhou Normal University, Hangzhou 311121, China; [c]GMU-GIBH Joint School of Life Sciences, Guangzhou Laboratory, Guangzhou Medical University, Guangzhou 510005, China; [d]Yongkang Maternity and Child Care hospital, Yongkang 321300, China; [e]Rutgers Cancer Institute of New Jersey, New Jersey, NJ 08901; [f]College of Animal Science and Technology, Nanjing Agricultural University, Nanjing 210095, China; and [g]Institute of Cancer Research, Shenzhen Bay Laboratory, Shenzhen 518107, China

1. D. Hoeller, C. M. Hecker, I. Dikic, Ubiquitin and ubiquitin-like proteins in cancer pathogenesis. *Nat. Rev. Cancer* **6**, 776–788 (2006).
2. L. Bedford, J. Lowe, L. R. Dick, R. J. Mayer, J. E. Brownell, Ubiquitin-like protein conjugation and the ubiquitin-proteasome system as drug targets. *Nat. Rev. Drug Discov.* **10**, 29–46 (2011).
3. M. Komatsu *et al.*, A novel protein-conjugating system for Ufm1, a ubiquitin-fold modifier. *EMBO J.* **23**, 1977–1986 (2004).
4. S. H. Kang *et al.*, Two novel ubiquitin-fold modifier 1 (Ufm1)-specific proteases, UfSP1 and UfSP2. *J. Biol. Chem.* **282**, 5256–5262 (2007).
5. Y. Gerakis, M. Quintero, H. Li, C. Hetz, The UFMylation system in proteostasis and beyond. *Trends Cell Biol.* **29**, 974–986 (2019).
6. D. Millrine *et al.*, Human UFSP1 is an active protease that regulates UFM1 maturation and UFMylation. *Cell Rep.* **40**, 1–21 (2022).
7. Q. Liang *et al.*, Human UFSP1 translated from an upstream near-cognate initiation codon functions as an active UFM1-specific protease. *J. Biol. Chem.* **298**, 1–11 (2022).
8. J. Liu *et al.*, A critical role of DDRGK1 in endoplasmic reticulum homoeostasis via regulation of IRE1alpha stability. *Nat. Commun.* **8**, 14186 (2017).
9. H. M. Yoo *et al.*, Modification of ASC1 by UFM1 is crucial for ER alpha transactivation and breast cancer development. *Mol. Cell* **56**, 261–274 (2014).
10. C. P. Walczak *et al.*, Ribosomal protein RPL26 is the principal target of UFMylation. *Proc. Natl. Acad. Sci. U.S.A.* **116**, 1299–1308 (2019).
11. C. M. Watson *et al.*, Beukes hip dysplasia segregates with a mutation identified in the UFM1-specific peptidase 2 gene, UFSP2. *Int. J. Exp. Pathol.* **91**, A17 (2010).
12. E. Colin *et al.*, Biallelic variants of UBA5 reveal that disruption of the UFM1 cascade can result in early-onset encephalopathy. *Eur. J. Hum. Genet.* **26**, 86–87 (2018).
13. H. F. Lu, Y. Yang, E. M. Allister, N. Wijesekara, M. B. Wheeler, The identification of potential factors associated with the development of type 2 diabetes: A quantitative proteomics approach. *Mol. Cell Proteomics* **7**, 1434–1451 (2008).
14. A. Azfer, J. L. Niu, L. M. Rogers, F. M. Adamski, P. E. Kolattukudy, Activation of endoplasmic reticulum stress response during the development of ischemic heart disease. *Am. J. Physiol. Heart Circ. Physiol.* **291**, H1411–H1420 (2006).
15. H. Liu *et al.*, Mallory-Denk Body (MDB) formation modulates ufmylation expression epigenetically in alcoholic hepatitis (AH) and non-alcoholic steatohepatitis (NASH). *Exp. Mol. Pathol.* **97**, 477–483 (2014).
16. Z. F. Wang *et al.*, MRE11 UFMylation promotes ATM activation. *Nucleic Acids Res.* **47**, 4124–4135 (2019).
17. B. Qin *et al.*, UFL1 promotes histone H4 ufmylation and ATM activation. *Nat. Commun.* **10**, 1–13 (2019).
18. J. Zhou *et al.*, Genomic profiling of the UFMylation family genes identifies UFSP2 as a potential tumour suppressor in colon cancer. *Clini. Transl. Med.* **11**, e642 (2021).
19. J. Liu *et al.*, UFMylation maintains tumour suppressor p53 stability by antagonizing its ubiquitination. *Nat. Cell Biol.* **22**, 1056–1063 (2020).
20. M. Zhang *et al.*, RCAD/Ufl1, a Ufm1 E3 ligase, is essential for hematopoietic stem cell function and murine hematopoiesis. *Cell Death Differ.* **22**, 1922–1934 (2015).
21. K. Tatsumi *et al.*, The Ufm1-activating enzyme Uba5 is indispensable for erythroid differentiation in mice. *Nat. Commun.* **2**, 1–7 (2011).
22. R. Yang *et al.*, CDK5RAP3, a UFL1 substrate adaptor, is crucial for liver development. *Development* **146**, 1–13 (2019).
23. Y. F. Cai *et al.*, UFBP1, a key component of the Ufm1 conjugation system, is essential for Ufmylation-mediated regulation of erythroid development. *PLoS Genet.* **11**, 1–21 (2015).
24. H. B. Zhu *et al.*, Ufbp1 promotes plasma cell development and ER expansion by modulating distinct branches of UPR. *Nat. Commun.* **10**, 1–15 (2019).
25. J. R. Liang *et al.*, A genome-wide ER-phagy screen highlights key roles of mitochondria!metabolism and ER-resident UFMylation. *Cell* **180**, 1160–1177 (2020).
26. J. Li *et al.*, Ufm1-specific ligase Ufl1 regulates endoplasmic reticulum homeostasis and protects against heart failure. *Circ. Heart Fail* **11**, e004917 (2018).
27. A. Xu, M. Barna, Cleaning up stalled ribosome-translocon complexes with ufmylation. *Cell Res.* **30**, 1–2 (2020).
28. R. DeJesus *et al.*, Functional CRISPR screening identifies the ufmylation pathway as a regulator of SQSTM1/p62. *Elife* **5**, e17290 (2016).
29. J. C. Wu, G. H. Lei, M. Mei, Y. Tang, H. L. Li, A novel C53/LZAP-interacting protein regulates stability of C53/LZAP and DDRGK domain-containing protein 1 (DDRGK1) and modulates NF-kappa B signaling. *J. Biol. Chem.* **285**, 15126–15136 (2010).
30. D. R. Balce *et al.*, UFMylation inhibits the proinflammatory capacity of interferon-gamma-activated macrophages. *Proc. Natl. Acad. Sci. U.S.A.* **118**, 1–10 (2021).
31. S. H. Baumeister, G. J. Freeman, G. Dranoff, A. H. Sharpe, Coinhibitory pathways in immunotherapy for cancer. *Annu. Rev. Immunol.* **34**, 539–573 (2016).
32. P. Sharma, J. P. Allison, The future of immune checkpoint therapy. *Science* **348**, 56–61 (2015).
33. V. A. Boussiotis, Molecular and biochemical aspects of the PD-1 checkpoint pathway. *New Engl. J. Med.* **375**, 1767–1778 (2016).
34. C. Sun, R. Mezzadra, T. N. Schumacher, Regulation and function of the PD-L1 checkpoint. *Immunity* **48**, 434–452 (2018).
35. J. R. Brahmer *et al.*, Safety and activity of Anti-PD-L1 antibody in patients with advanced cancer. *New Engl. J. Med.* **366**, 2455–2465 (2012).
36. M. Santoni, R. Montironi, N. Battelli, Immune checkpoint blockade in advanced renal-cell carcinoma. *New Engl. J. Med.* **379**, 91–93 (2018).
37. A. Snyder *et al.*, Contribution of systemic and somatic factors to clinical response and resistance to PD-L1 blockade in urothelial cancer: An exploratory multi-omic analysis. *PLoS Med.* **14**, 1–24 (2017).
38. B. H. Moreno, G. Parisi, L. Robert, A. Ribas, Anti-PD-1 therapy in melanoma. *Semin. Oncol.* **42**, 466–473 (2015).
39. L. Galluzzi, T. A. Chan, G. Kroemer, J. D. Wolchok, A. Lopez-Soto, The hallmarks of successful anticancer immunotherapy. *Sci. Transl. Med.* **10**, 1–14 (2018).
40. J. M. Chinai *et al.*, New immunotherapies targeting the PD-1 pathway. *Trends Pharmacol. Sci.* **36**, 587–595 (2015).
41. A. V. R. Kornepati, R. K. Vadlamudi, T. Curie, Programmed cell death 1 ligand 1 signals in cancer cells. *Nat. Rev. Cancer* **22**, 174–189 (2022).
42. J. F. Zhang, F. B. Dang, J. M. Ren, W. Y. Wei, Biochemical aspects of PD-L1 regulation in cancer immunotherapy. *Trends Biochem. Sci.* **43**, 1014–1032 (2018).
43. W. P. Zou, J. D. Wolchok, L. P. Chen, PD-L1 (B7–H1) and PD-1 pathway blockade for cancer therapy: Mechanisms, response biomarkers, and combinations. *Sci. Transl. Med.* **8**, 1–14 (2016).
44. S. O. Lim *et al.*, Deubiquitination and stabilization of PD-L1 by CSN5. *Cancer Cell* **30**, 925–939 (2016).
45. C. W. Li *et al.*, Glycosylation and stabilization of programmed death ligand-1 suppresses T-cell activity. *Nat. Commun.* **7**, 1–11 (2016).
46. J. H. Cha *et al.*, Metformin promotes antitumor immunity via endoplasmic-reticulum-associated degradation of PD-L1. *Mol. Cell* **71**, 606–620 (2018).
47. Y. Gao *et al.*, Acetylation-dependent regulation of PD-L1 nuclear translocation dictates the efficacy of anti-PD-1 immunotherapy. *Nat. Cell Biol.* **22**, 1064–1095 (2020).
48. H. Yao *et al.*, Inhibiting PD-L1 palmitoylation enhances T-cell immune responses against tumours. *Nat. Biomed. Eng.* **3**, 306–317 (2019).
49. Y. Yang *et al.*, Palmitoylation stabilizes PD-L1 to promote breast tumor growth. *Cell Res.* **29**, 83–86 (2019).
50. I. Braakman, N. J. Bulleid, Protein folding and modification in the mammalian endoplasmic reticulum. *Annu. Rev. Biochem.* **80**, 71–99 (2011).
51. J. M. Hsu, C. W. Li, Y. J. Lai, M. C. Hung, Posttranslational modifications of PD-L1 and their applications in cancer therapy. *Cancer Res.* **78**, 6349–6353 (2018).
52. D. S. Schwarz, M. D. Blower, The endoplasmic reticulum: Structure, function and response to cellular signaling. *Cell Mol. Life Sci.* **73**, 79–94 (2016).
53. J. H. Cha, L. C. Chan, C. W. Li, J. L. Hsu, M. C. Hung, Mechanisms controlling PD-L1 expression in cancer. *Mol. Cell* **76**, 359–370 (2019).
54. K. Lemaire *et al.*, Ubiquitin fold modifier 1 (UFM1) and its target UFBP1 protect pancreatic beta cells from ER stress-induced apoptosis. *PLoS One* **6**, 1–14 (2011).
55. S. Hanzelmann, R. Castelo, J. Guinney, GSVA: Gene set variation analysis for microarray and RNA-seq data. *BMC Bioinformatics* **14**, 1–15 (2013).
56. M. Harel *et al.*, Proteomics of melanoma response to immunotherapy reveals mitochondrial dependence. *Cell* **179**, 236–250 (2019).
57. J. Zhou *et al.*, Optimized protocol to detect protein UFMylation in cells and in vitro via immunoblotting. *STAR Protoc.* **3**, 1–12 (2022).
58. M. L. Burr *et al.*, CMTM6 maintains the expression of PD-L1 and regulates anti-tumour immunity. *Nature* **549**, 101–105 (2017).
59. H. B. Wang *et al.*, HIP1R targets PD-L1 to lysosomal degradation to alter T cell-mediated cytotoxicity. *Nat. Chem. Biol.* **15**, 42–50 (2019).
60. J. F. Zhang *et al.*, Cyclin D-CDK4 kinase destabilizes PD-L1 via cullin 3-SPOP to control cancer immune surveillance. *Nature* **553**, 91–120 (2018).
61. S. H. Baumeister, G. J. Freeman, G. Dranoff, A. H. Sharpe, Coinhibitory pathways in immunotherapy for cancer. *Annu. Rev. Immunol.* **34**, 539–573 (2016).
62. I. S. Afonina, S. P. Cullen, S. J. Martin, Cytotoxic and non-cytotoxic roles of the CTL/NK protease granzyme B. *Immunol. Rev.* **235**, 105–116 (2010).